The Dipole Moment Derivatives of Methane

Kwan Kim* and Cheol Woo Park

Department of Chemistry, College of Natural Sciences, Seoul National University, Seoul 151

Received July 10, 1986

The infrared intensities of CH_4 and CD_4 are analyzed. The experimental dipole moment derivatives thus obtained are compared with corresponding values from the molecular orbital calculations. The theoretical results are analyzed for the charge-charge flux-overlap(CCFO) electronic contributions to the dipole derivatives.

Introduction

Infrared spectroscopy is an ancient field of study. Its modern phase dates back well over 100 years. For most of that time it has been recognized that the study of vibrational intensities is an interesting and desirable thing to do. Nevertheless, this study has been at much less depth than has the corresponding study of the frequencies of absorption in vibrational spectra of molecules. We believe that one important reason that more work in vibrational intensities has not been done is that the interpretation of these results has not been easy.

In this last decade much effort has been devoted to the interpretation of infrared intensities, and much progress has been attained in using them to obtain information about the electronic distribution in molecules.[1] The search for correlations between intensity parameters and chemical behavior has been considerable, and several partitioning schemes of the total dipole moment derivatives have appeared. Among such schemes, we find the atomic polar tensor formalism[2] particularly convenient. In addition, splitting of atomic polar tensor elements into charge, charge flux and overlap contributions has proved a useful way to analyze the infrared intensities in terms of the electronic structure changes taking place during vibrational motions.[3]

Recently we reported the infrared band intensities of methane (CH_4 and CD_4)[4], a molecule that has received considerable attention in the past due to its importance in astrophysical studies as well as in understanding molecular structure.[5] In this paper we analyze those results. From the observed intensities a set of dipole moment derivatives has been obtained. The magnitudes and signs of the derivatives are compared with the semi-empirical and ab initio calculated results. The dipole moment derivatives have been transformed into the atomic polar tensors. The polar tensor elements are also analyzed in terms of the quantum mechanical charge, charge flux and overlap (CCFO) model.[6] In addition, the fundamental intensities of CH_3D and CD_3H are predicted, and compared with the previously reported values.

IR Intensities and Polar Tensor

Details of the infrared intensities and polar tensors have been described previously.[6] Briefly, in the rigid rotor harmonic oscillator approximation, the integrated molar infrared absorption coefficients, A_i, for the i-th fundamental band is expressed as follows,[7]

$$\left(\frac{A_i}{\text{km}\cdot\text{mol}^{-1}}\right) = (974.8644)d_i\left|\frac{(\partial P/\partial Q_i)}{eu^{-1/2}}\right|^2 \quad (1)$$

Here, d_i is the degeneracy of the i-th fundamental vibrational mode, $\partial P/\partial Q_i$ is the vector dipole moment derivative with respect to the i-th normal coordinate, e is the electronic charge, and u is the atomic mass unit.

A polar tensor in normal coordinate space, P_Q, is defined as follows[8] for a molecule having 3n-6 fundamental vibrational modes:

$$P_Q = \begin{bmatrix} \partial P_x/\partial Q_1 & \partial P_x/\partial Q_2 & \cdots & \partial P_x/\partial Q_{3n-6} \\ \partial P_y/\partial Q_1 & \partial P_y/\partial Q_2 & \cdots & \partial P_y/\partial Q_{3n-6} \\ \partial P_z/\partial Q_1 & \partial P_z/\partial Q_2 & \cdots & \partial P_z/\partial Q_{3n-6} \end{bmatrix} \quad (2)$$

The transformation to space-fixed Cartesian coordinates can be applied to obtain the "polar tensor in Cartesian coordinate space"[6], P_x

$$P_x = P_Q L^{-1} U B + P_\rho \beta \quad (3)$$

Here L^{-1} is the inverse of a normal coordinate transformation matrix between the internal symmetry coordinates, S_i, and the normal coordinates, Q_i, ($S=LQ$), U is a transformation matrix between the symmetry coordinates and the internal coordinates, R_k, ($S=UR$), B is a transformation matrix between the internal coordinates and the space-fixed Cartesian displacement coordinates, X_r, ($R=BX$), and $P_\rho\beta$ is a rotation correction to P_x.

Notice that P_x is the juxtaposition of n 3×3 "atomic polar tensors"[2] P_x^α

$$P_x^\alpha = \begin{bmatrix} \partial P_x/\partial x_\alpha & \partial P_x/\partial y_\alpha & \partial P_x/\partial z_\alpha \\ \partial P_y/\partial x_\alpha & \partial P_y/\partial y_\alpha & \partial P_y/\partial z_\alpha \\ \partial P_z/\partial x_\alpha & \partial P_z/\partial y_\alpha & \partial P_z/\partial z_\alpha \end{bmatrix} \quad (4)$$

Here x_α, y_α, z_α are the space-fixed Cartesian displacement coordinates of the α-th atom and P_x, P_y, P_z are the components of the total dipole moment of the molecule on the space-fixed axes. When these atomic polar tensors (here after abbreviated as APTs) are juxtaposed in the order dictated by the definition of B and X, we obtain the polar tensor of the molecule,

$$P_x = \{P_x^1 \vdots P_x^2 \vdots \cdots \vdots P_x^\alpha \vdots \cdots \vdots P_x^n\} \quad (5)$$

This matrix is another representation of the experimental intensity information, transformed by the normal coordinate transformations. Although the general expression for P_x given above apparently has a very large number ($3\times3n$) of elements, many of them are zeroes. For molecules with some symmetry, the APTs will reflect the symmetry.[3] For example, if an atom lies on an axis with three-fold or greater symmetry, the APT is diagonal. The APTs for atoms related by symmetry will also be related. For example, the APT for the H(2) atom, P_x^{H2},

in CH_4 (See Figure 1) is diagonal and the APTs for other H atoms, P_x^*, are related with P_x^{H2}, by $P_x^* = T P_x^{H2} T'$, where T is a transformation matrix (T' is its transpose) from the original molecular axes used in obtaining the P_x^{H2} to the new rotated bond coordinate axes whose function to the α atom is same as the original coordinate axes to H(2) atom. In addition, since the APTs for all the atoms in CH_4 are related by $\sum_q P_x^q = 0$ (null tensor)[3], there are only three independent intensity parameters for the APTs of the five atoms in CH_4. Moreover, in methane $\partial P_x/\partial x$ is equal to $\partial P_y/\partial y$ for the H(2) atom due to the spherical symmetry of the molecule. Hence, only two elements are needed to specify all the APTs of methane.

We may also transform P_x to P_Q by using the inverse relation of equation (3), that is,

$$P_Q = P_x A U' L \tag{6}$$

Here the matrix A is the inverse transformation from internal coordinates to Cartesian coordinates, defined so that $BA = I$, a square identity matrix. Other symbols have their customary meaning as used above. Equation (6) has particular interest in that it is especially easy to calculate the polar tensor P_x from quantum mechanical procedures.

The polar tensor values of methane have been calculated

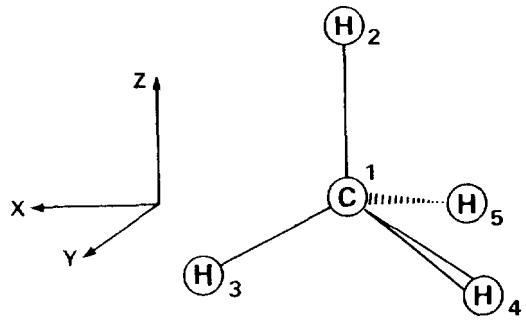

Figure 1. Coordinate axes and molecular orientation of methane used in normal coordinate calculation.

Table 1. Structural Data and Definition of Internal and Symmetry Coordinates of Methane

Masses(u)[a]: $m_C = 12.0$ $m_H = 1.007825$ $m_D = 2.014102$

Structure[b]: $R_{CH} = 0.1091$ nm

Internal coordinates[c]:

$R_1 = \delta r_{12}$	$R_6 = \delta\alpha_{214}$
$R_2 = \delta r_{13}$	$R_7 = \delta\alpha_{215}$
$R_3 = \delta r_{14}$	$R_8 = \delta\alpha_{415}$
$R_4 = \delta r_{15}$	$R_9 = \delta\alpha_{314}$
$R_5 = \delta\alpha_{213}$	$R_{10} = \delta\alpha_{315}$

Symmetry coordinates[d]:

C_{3v}	T_d	
A_1	A_1	$S_1 = (1/2)(R_1 + R_2 + R_3 + R_4)$
	F_2	$S_2 = (1/\sqrt{12})(3R_1 - R_2 - R_3 - R_4)$
		$S_3 = (1/\sqrt{6})(R_5 + R_6 + R_7 - R_8 - R_9 - R_{10})$
E_x	E_x	$S_4 = (1/\sqrt{12})(2R_6 - R_8 - R_7 + 2R_8 - R_9 - R_{10})$
	F_x	$S_5 = (1/\sqrt{6})(2R_2 - R_3 - R_4)$
		$S_6 = (1/\sqrt{12})(2R_5 - R_6 - R_7 - 2R_8 + R_9 + R_{10})$
E_y	E_y	$S_7 = (1/2)(R_6 - R_7 - R_9 + R_{10})$
	F_y	$S_8 = (1/\sqrt{2})(R_3 - R_4)$
		$S_9 = (1/2)(R_6 - R_7 + R_9 - R_{10})$
A_1	A_1	$S_{red} = (1/\sqrt{6})(R_5 + R_6 + R_7 + R_8 + R_9 + R_{10})$

[a]Ref. (10), [b]Ref. (11), [c]The subscripts refer to the atoms shown in Figure 1; r_{ij} is a C_i–H_j bond and α_{ijk} is a $H_i C_j H_k$ angle, [d]S_{red} is a redundant coordinate.

Table 2. Harmonic Force Field, Normal Coordinates, and Integrated Intensities of Methane

Harmonic force constants (Nm^{-1})[a]:

A_1	$K_{11} = 584.2$	F	$K_{33} = 538.3$
E	$K_{22} = 57.8$		$K_{34} = 22.5$
			$K_{44} = 54.5$

Normal coordinates ($u^{-1/2}$)[b]:

CH_4 F_x[c]

	Q_3	Q_4
S_2	1.0496	−0.0405
S_3	−0.1392	1.4217

CD_4 F_x[c]

	Q_3	Q_4
S_2	0.7794	−0.0105
S_3	−0.2469	1.0708

CH_3D[d] A_1

	Q_1	Q_2	Q_3
S_1	0.8482	0.3856	0.0107
S_2	−0.5503	0.6544	−0.0220
S_3	0.0739	−0.2017	1.4123

E_x[e]

	Q_4	Q_5	Q_6
S_4	−0.0105	1.4055	0.4615
S_5	1.0498	0.0181	−0.0314
S_6	−0.1490	−0.6037	1.1583

CD_3H[f] A_1

	Q_1	Q_2	Q_3
S_1	0.4751	0.6282	−0.0084
S_2	0.9229	−0.3565	−0.0234
S_3	−0.1453	0.1243	1.0822

E_x[g]

	Q_4	Q_5	Q_6
S_4	0.0059	1.0805	−0.6294
S_5	0.7794	−0.0094	−0.0089
S_6	−0.2413	0.8121	0.8957

Intensities ($km \cdot mol^{-1}$)[a]

CH_4	$A_3(\nu_3) = 66.82 \pm 0.22$	$A_4(\nu_4) = 32.72 \pm 0.54$
CD_4	$A_3(\nu_3) = 29.83 \pm 0.85$	$A_4(\nu_4) = 19.03 \pm 0.63$

[a]Ref. (9); [b]The indices labelling the normal coordinates correspond to the labels identifying the vibrational mode given in ref. (12).; [c]The K and L elements for the F_x and F_y blocks are identical with those of F_x block; [d]The D atom corresponds to the H(2) atom in Figure 1. [e]The L elements for the E_y block are identical with those of E_x block. E_x in C_{3v} point group corresponds to the combination of E_x and F_x in T_d point group. See the definition of symmetry coordinates in Table 1; [f]The H atom corresponds to the H(2) atom in Figure 1.; [g]Taken from ref. (4). The indices labelling the vibrational modes correspond to the notations given in footnote (b) above.

by means of equation (3) using the intensity data[4] we reported recently. The Cartesian coordinate axes, numbering of atoms, and orientation of methane molecule are shown in Figure 1. The equilibrium structural data, and the definition of the internal and symmetry coordinates are listed in Table 1. The L matrices were calculated using the harmonic force field reported by Duncan *et al.*[9]. These values are given in Table 2. The B matrix was evaluated using Wilson's method[7]. In Table 3 representative values for the atomic polar tensors of CH_4 and CD_4 are given for the C(1), H(2), and H(3) atoms of Figure 1. The experimental errors for the individual polar tensor elements are given in parenthesis.

The experimental infrared intensities are proportional to the square of the dipole moment derivatives with respect to the normal coordinates of the molecule, $\partial P/\partial Q_i$ (see eq. (1)). Hence, the atomic polar tensor elements are given in Table 3 for all possible sign combinations of the $\partial P/\partial Q_i$ quantities. Comparison of the values of polar tensors for CH_4 and CD_4 leads to the (+, +) or (−, −) sign combinations for the $\partial P/\partial Q_i$'s.

In order to reach some decision about which of the several possible polar tensors are correct for methane, we may compare the different possible sets of the P_x values from the experimental data with the quantum mechanically calculated

Table 3. Atomic Polar Tensors of Methane in Units of e's

		P_x^C			$P_x^{H(2)}$[c]			$P_x^{H(3)}$		
CH_4[a]		∓0.012[d] (0.002)	0	0	∓0.063 (0.001)	0	0	±0.112 (0.001)	0	∓0.062 (0.001)
	+ +[b]	0	∓0.012 (0.002)	0	0	∓0.063 (0.001)	0	0	∓0.063 (0.001)	0
	− −	0	0	∓0.012 (0.002)	0	0	±0.134 (0.001)	∓0.062 (0.001)	0	∓0.041 (0.001)
		∓0.305 (0.002)	0	0	±0.056 (0.001)	0	0	±0.110 (0.001)	0	∓0.019 (0.001)
	+ −	0	∓0.305 (0.002)	0	0	±0.056 (0.001)	0	0	±0.056 (0.001)	0
	− +	0	0	∓0.305 (0.002)	0	0	±0.117 (0.001)	∓0.019 (0.001)	0	±0.063 (0.001)
CD_4[a]		∓0.015 (0.005)	0	0	∓0.061 (0.001)	0	0	±0.112 (0.002)	0	∓0.061 (0.001)
	+ +	0	∓0.015 (0.005)	0	0	∓0.061 (0.001)	0	0	∓0.061 (0.001)	0
	− −	0	0	∓0.015 (0.005)	0	0	±0.133 (0.002)	∓0.061 (0.001)	0	∓0.039 (0.001)
		∓0.280 (0.005)	0	0	±0.059 (0.001)	0	0	±0.088 (0.002)	0	∓0.010 (0.001)
	+ −	0	∓0.280 (0.005)	0	0	±0.059 (0.001)	0	0	±0.059 (0.001)	0
	− +	0	0	∓0.280 (0.005)	0	0	±0.092 (0.002)	∓0.010 (0.001)	0	±0.063 (0.001)
		0.033	0	0	0.004	0	0	−0.095	0	0.049
	CNDO/2[e]	0	0.033	0	0	0.044	0	0	0.044	0
		0	0	0.033	0	0	−0.113	0.049	0	0.026
		0.180	0	0	0.004	0	0	−0.127	0	0.046
CH_4	INDO[e]	0	0.180	0	0	0.004	0	0	0.004	0
and		0	0	0.180	0	0	−0.143	0.046	0	−0.012
		−0.074	0	0	0.043	0	0	−0.023	0	0.023
CD_4	STO-3G[f]	0	−0.074	0	0	0.043	0	0	0.043	0
		0	0	−0.074	0	0	−0.031	0.023	0	0.035
		0.010	0	0	0.085	0	0	−0.149	0	0.083
	6-31G[f]	0	0.010	0	0	0.085	0	0	0.085	0
		0	0	0.010	0	0	−0.178	0.083	0	0.056

[a]Intensities given in Table 2 were used in this calculation; [b]The signs are the signs of the $\partial P/\partial Q_i$'s. For example, (±±) would mean that the signs of $\partial P/\partial Q_3$ and $\partial P/\partial Q_4$ are both either positive or negative; [c]The atomic polar tensor of H(or D) atom numbered as 2 in Figure 1; [d]The value with upper sign(−0.012) is, for example, the tensor elements obtained from the signs of $\partial P/\partial Q_i$'s corresponding to the upper sign combination(+ +) in two sets of sign choices(±±). The value in parenthesis represents the uncertainty based on the estimated errors in the reported intensities and the harmonic force fields; [e]These tensors were calculated using the CNINDO program 141 from QCPE; [f]Calculated by using the GAUSSIAN 70 PROGRAM (see ref. 13).

values. In the present work, the dipole moment derivatives have been calculated by the CNDO/2, INDO, and ab initio quantum mechanical methods, and the results are also given in Table 3. In view of the quantum mechanically calculated values, the (−, −) sign combination has to be chosen. Although the differences between the dipole moment derivatives calculated by different methods are quite large, they all show the same signs. As usual, the 6-31G ab initio and CNDO/2 results are superior to the STO-3G and INDO results. The work of Meyer *et al.*[14] clearly demonstrated the basis-set sensitivity of the calculated values of the dipole moment derivatives and the limited success to predict reliable values for these quantities by quantum mechanical methods.

The close correspondence between the values of polar tensors for CH_4 and CD_4 reflects the consistency of our reported[4] intensity data. As a further check on the quality of our tensor elements obtained from the CH_4 and CD_4 intensities the absolute intensities for the isotopic series CH_3D and CD_3H have been calculated by using the mean values of Table 3. In this calculation, the relation of equation(6) was used. The results are shown in Table 4 together with the corresponding observed values of Saeki *et al.*[15] and those of Hiller *et al.*[16]. Comparing the experimental values for CH_3D and CD_3H of both Hiller *et al.* and Saeki *et al.* with our predicted values, we found a very satisfactory correspondence.

From the values of the H(2) polar tensor it can be seen that as the CH bond bends along the positive x(or y) coordinate, the negative charges on carbon move to the negative x(or y) direction resulting in a positive contribution to the dipole moment derivatives. On the other hand, as the CH bond stretches along the positive z coordinates, the negative charges on carbon move to the positive z direction exhibiting a negative contribution to the dipole derivative. It should be noticed, however, that above explanations are accurate wholly on the classical atomic charge model. As will be clear in the following CCFO analysis of APT elements, a quantum mechanical interference term, which has no classical analogue, contributes excessively large to the atomic polar tensor. Hence the movement of negative charge during molecular vibration should be understood merely on the conceptual basis.

Table 4. Observed and Predicted Intensities for CH_3D and CD_3H in Units of km-mol^{-1}'s

	Vib freq[a]	Obsd int		Calcd int
	(cm^{-1})	Hiller *et al.*[b]	Saeki *et al.*[c]	this work
CH_3D	ν_1 2970	49.2	49.3	50.9
	ν_4 3017			
	ν_2 2200	6.3	6.1	7.1
	ν_3 1307			
	ν_5 1471	29.3	31.4	29.2
	ν_6 1161			
CD_3H	ν_1 2992	15.7	15.8	16.9
	ν_2 2143	21.0	20.2	22.4
	ν_4 2251			
	ν_5 1291	6.7	6.6	7.4
	ν_3 1003	15.3	14.7	15.6
	ν_6 1036			

[a]Ref(17). [b]Ref(16). [c]Ref(15)

CCFO analysis of APT elements

Details of the charge-charge flux-overlap electronic contributions to the dipole derivatives have been described previously.[3] Briefly, the atomic polar tensor can be identified with three contributing terms.

$$P_I^\alpha = \zeta_\alpha I + \sum_\beta (\nabla_\alpha \zeta_\beta) R_\beta - \sum_\beta \nabla_\alpha \Phi_{\beta\beta}(R) \qquad (7)$$

The first term is the contribution of a "net charge" fixed on the nucleus, and the second is the "charge–flux" contribution from the transfer of charge from one nucleus to another as the result of nuclear displacement. The third term is strictly a quantum mechanical contribution resulting from the superposition of wave functions, and has no classical analogue. By assessing the relative importance of each of these three contributions for a given tensor it is possible that valuable chemical information may be obtained.[18]

Table 5 shows the CNDO/2, INDO semi-empirical and STO-3G, 6-31G ab-initio atomic polar tensors for the H(2) atom of Figure 1 in CH_4. Regardless of the basis sets, it can be seen from the Table that all three of the constituent parts of the polar tensor, defined in equation (7) are significant. None of the three groups of terms can be completely neglected. The semi-empirical results (CNDO/2 and INDO) exhibit, however, that the net charge contribution, $\zeta_H I$, is far less than those from the remaining two terms. On the other hand, all three terms contribute more or less equally in the ab-initio calculations (STO-3G and 6-31G). Particularly noteworthy in common is the large charge flux contributions. This represents a large charge transfer along the CH bond during the stretching (←C–H→), and is indicative of the considerable electronic rearrangement that takes place as this bond is broken. Also it appears from the Table that the equilibrium bond dipole has the polarity of $^-$CH–H$^+$. A negative value of the charge-flux contribu-

Table 5. Comparison of Hydrogen Polar Tensors in CH_4 Obtained by Quantum Mechanical Calculations and by Experiment, in Natural Units(e)[a]

		$\partial P_x/\partial x_H (= \partial P_y/\partial y_H)$	$\partial P_z/\partial z_H$
$\zeta_H I$	CNDO/2	0.013	0.013
	INDO	−0.009	−0.009
	STO-3G	0.063	0.063
	6-31G	0.155	0.155
$\sum_\alpha \nabla_H \zeta_\alpha R_\alpha$	CNDO/2	−0.046	−0.093
	INDO	−0.051	−0.101
	STO-3G	−0.033	−0.166
	6-31G	−0.033	−0.185
$-\sum_\alpha \nabla_H \Phi_{\alpha\alpha}$	CNDO/2	0.077	−0.033
	INDO	0.064	−0.033
	STO-3G	0.013	0.072
	6-31G	−0.037	−0.148
APT of H(2)[b]	CNDO/2	0.044	−0.113
	INDO	0.004	−0.143
	STO-3G	0.043	−0.031
	6-31G	0.085	−0.178
	expt'l	0.062	−0.134

[a]APT for the H(2) atom of Figure 1; [b]See Table 3.

tion would indicate that the hydrogen end of the bond dipole becomes negatively charged as the C–H length is increased.

The relatively large value of the quantum mechanical interference term reflects that there occurs significant changes in the hybridization scheme during the molecular vibration. Hence it seems that the classical atomic charge model, like that proposed by Decius,[19] may not be valid for interpreting infrared intensities. Although the present results show that the calculated values of the three terms in equation (7) are sensitive to the basis-set, it seems rather encouraging that the simple semi-empirical CNDO/2 method is superior to the INDO and STO-3G ab-initio methods in the vibrational intensity analysis.

At the end of previous section it was pointed out that the movement of negative charges during molecular vibration should be understood merely on the conceptual basis. Concept of such a charge-movement is directly related with both the net charge and the charge-flux contributions. As can be seen from Table 5, all the values of APT elements due to either the net charge or the charge flux terms have same signs regardless of the quantum-mechanical basis-sets, whereas the elements of $P_x^{H_2}$ do have opposite signs. That is, the sign of $\partial P_x/\partial x_H (= \partial P_y/\partial y_H)$ is opposite to that of $\partial P_x/\partial z_H$. It is evident from Table 5 that the large negative value of $\partial P_x/\partial z$ in $P_x^{H_2}$ of methane arises from the composite effect of both the charge flux and the overlap (interference) contributions. On the other hand, for the $\partial P_x/\partial x (= \partial P_y/\partial y)$ element the net charge and/or the overlap contributions dominate such that the element becomes positive. Hence, none of the three groups of terms in equation (7) seems to be completely neglected in the vibrational intensity analysis. Care should thus be paid whenever one interprets infrared intensities in terms of classical models.

Conclusion

We have analyzed the infrared intensities of CH_4 and CD_4. The experimentally derived polar tensors for the H and C atoms in CH_4 and CD_4 were in essentially exact agreement with one another. The polar tensors derived by the quantum mechanical calculations were also in fair agreement with the experimental results although there were some discrepancy in the magnitudes. Not only were the polar tensors from CH_4 and from CD_4 in closest agreement, but the band intensities of CH_3D and CD_3H computed from the CH_4 and CD_4 polar tensors were close to their experimental values. These observations may indicate that our recent measurement[4] on the infrared intensities of methane was extremely precise.

From the quantum mechanical calculation partitioning the polar tensor elements into the charge-charge flux-overlap parts, the charge flux contribution was found to be most important. Nevertheless, APT appeared to depend significantly upon the nonclassical overlap (interference) term. Although the theoretical results are very sensitive to the basis-sets, the CNDO/2 method seems to be highly successful for the calculation of infrared intensities comparing favorably with ab initio calculation. It is, of course, hoped that this is borne out by calculations on other species of interest.

Acknowledgement. This work was supported in part by the Korea Science and Engineering Foundation.

References

1. W.B. Person and G. Zerbi, Eds., "Vibrational Intensities in Infrared and Raman Spectroscopy", Elsevier, Amsterdam (1982).
2. W.B. Person and J.H. Newton, *J. Chem. Phys.* **61**, 1040 (1974).
3. K. Kim and H.G. Lee, *Bull. Kor. Chem. Soc.* **6**, 79 (1985).
4. K. Kim, *J. Quant. Spectrosc. Radia. Transfer,* in press.
5. W.T. King and G.B. Mast, *J. Phys. Chem.*, **80**, 2521 (1976).
6. K. Kim, *Bull. Kor. Chem. Soc.* **6**, 158 (1985).
7. E.B. Wilson, Jr., J.C. Decius, and P.C. Cross, "Molecular Vibrations", McGraw-Hill, New York (1955).
8. W.B. Person and D. Steele, *Mol. Spectrosc.* **2**, 357 (1974).
9. J.L. Duncan and I.M. Mills, *Spectrochim. Acta* **20**, 523 (1964).
10. A.H. Wapstra and N.B. Gove, *Nucl. Data Tables* **A9**, 265 (1971).
11. L.E. Sutton, "Interatomic Distances", The Chemical Society, London (1958).
12. J.H.F. Bode and W.M.A. Smit, *J. Phys. Chem.* **84**, 198(1980).
13. W.J. Hehre, W.A. Latham, R. Ditchfield, M.D. Newton, and J.A. Pople, *Quantum Chem. Program Exchange,* QCPE **10**, 236(1974).
14. W. Meyer and P. Pulay, *J. Chem. Phys.* **56**, 2109 (1972).
15. S. Saeki, M. Mizuno, and S. Kondo, *Spectrochim. Acta* Part **A32**, 403(1976).
16. R.E. Hiller, Jr., and J.W. Straley, *J. Mol. Spectrosc.* **5**, 24(1960).
17. D.L. Gray and A.G. Robiette, *Mol. Phys.* **37**, 1901(1979).
18. M.N. Ramos and B.B. Neto, *J. Mol. Struct,* **140**, 107(1986).
19. J.C. Decius, *J. Mol. Spectrosc.* **57**, 348(1975).